

Received April 9, 2019, accepted May 6, 2019, date of publication May 22, 2019, date of current version June 10, 2019.

Digital Object Identifier 10.1109/ACCESS.2019.2918338

# Optical-RoI-Signaling for Vehicular Communications

MINH DUC THIEU<sup>1</sup>, TUNG LAM PHAM<sup>1</sup>, TRANG NGUYEN<sup>1</sup>,  
AND YEONG MIN JANG<sup>1</sup>, (Member, IEEE)

Department of Electronics Engineering, Kookmin University, Seoul 02707, South Korea

Corresponding author: Yeong Min Jang (yjang@kookmin.ac.kr)

This work was supported by the Institute for Information and Communications Technology Promotion (IITP) through the Korean Government (MSIP) — Development of Intelligent and Hybrid OCC-LiFi Systems for Next Generation Optical Wireless Communications under Grant 2017-0-00824.

**ABSTRACT** This paper introduces a new hybrid waveform for optical wireless communication (OWC)/optical camera communication (OCC) systems and discusses the technical considerations of these systems. In a challenged vehicular communication environment, which requires high-speed, high-mobility, and long-distance communication support, implementing a hybrid waveform guarantees high-speed data transmission while reducing the cost of the OWC/OCC systems. The application of a hybrid waveform in the OWC/OCC systems is known as the region-of-interest (RoI)-signaling technique. This technique allows the OWC/OCC systems to simultaneously transmit low-rate and high-rate data streams. The low-rate data stream is used to detect and track the RoI of light sources for setting up the communication link, whereas the high-rate data stream is used for high-speed data transmission. Selection of proper modulation schemes for two simultaneous data streams is also discussed in this paper. A new modulation scheme, such as spatial-2-phase-shift-keying (S2-PSK), is proposed for the low-rate data stream. This scheme has been used to modify the IEEE 802.15.7-2018 standard, which is the revised version of the IEEE 802.15.7-2011 standard. For the high-rate data stream, single-carrier modulation or multiple-carrier modulation, such as the proposed hybrid-spatial-phase-shift-keying (HS-PSK) or variable pulse-position modulation (VPPM), can serve as viable solutions. Technical considerations for the modulation schemes of each type of data stream are analyzed to determine the feasibility of the proposed schemes. Finally, the experimental results and numerical parameters of the intended system are presented.

**INDEX TERMS** Optical wireless communication (OWC), optical camera communication (OCC), vehicular communications, IEEE 802.15.7-2018, spatial-2-phase-shift-keying (S2-PSK), hybrid-spatial-phase-shift-keying (HS-PSK), dimming-spatial-8-phase-shift-keying (DS8-PSK), Internet of vehicles (IoV), V2X communications.

## I. INTRODUCTION

In recent years, the number of studies on vehicle-to-vehicle (V2V) and vehicle-to-infrastructure (V2I) communication for vehicles has increased rapidly due to the increasing demand for safe driving and mitigation of traffic congestion. According to [1], by 2020, more than 90% of cars sold will be connected. Therefore, developing vehicle-to-everything (V2X) communication technologies promises entry into a hugely profitable market within the automotive industry, which can enhance traffic safety more efficiently. Due to the increasing demand for wireless data communication, current

conventional radio frequency (RF)-based communication networks would not be able to fully satisfy the network traffic growth requirements in the future [2]. Therefore, new wireless communication technologies are required to fill this gap. However, the usage of these new technologies should not exclude RF communication, and they should be fully compatible with each other in all circumstances.

The advantages of visible light communication (VLC) and optical wireless communication (OWC)/optical camera communication (OCC) over existing RF communication have been discussed recently [2]–[5]. These advantages can be summarized as follows:

- The available bandwidth range of visible light (approximately 430–770 THz) is more than about

The associate editor coordinating the review of this manuscript and approving it for publication was Bora Onat.

1000 times the bandwidth of the entire RF spectrum (approximately 300 GHz).

- RF can bring harmful effects to human health if the transmission power is beyond the specific limit.
- There is no cost for using visible light spectra because they are not regulated. In addition, given the support from existing lighting infrastructures on streets and in vehicles, the cost of implementing VLC and OWC/OCC systems is lower compared with the cost of installing RF units on roads.
- In many circumstances, RF suffers from interferences between non-line-of-sight (nLoS) systems due to the electromagnetic wave properties.

Light-emitting diodes (LEDs) are expected to be used as next-generation lighting sources owing to their advantages, such as good visibility, long life, and low-power consumption. The ability of LEDs to switch light intensity at a fast rate [6], [7] has led to the high-speed data transmission capacity of transmitters in VLC and OWC/OCC systems. On the receiver side, VLC and OWC/OCC systems use different types of light receivers [3]. Cameras are used in the OWC/OCC system to receive modulated light, whereas photodiodes are used in the VLC system. Moreover, cameras are used for safety and comfort applications in the automotive field. Hence, VLC and OWC/OCC are candidates for use in V2X communication, providing safety assistance solutions based on communication.

RF technologies still play an important role in V2X communication. Currently, 5G mobile communication networks are also expected to be used in future vehicular communication systems. Hence, some studies have investigated the system model, performance, and software architecture of vehicular networks using 5G (e.g., [8] and [9]). On the other hand, the Internet of Vehicles (IoV) is currently of high interest inspired by the concept of the Internet of Things (IoT). Its benefits, comprehensive framework, and challenges were discussed in [10]. The Vehicular Cyber-Physical System (VCPS) is also considered as a new paradigm for vehicular communications [10] due to the growing importance of cloud-based intelligent computation in big traffic data. Hence, the proposed architecture and network model of IoV should support VCPS as the next generation of the Internet.

In our recent papers (i.e., [3], [11], and [12]), we proposed a hybrid system and investigated OCC that involved high-frame-rate camera processing to accelerate the data rate. In the present paper, we discuss the vehicular OCC system, which is a combination of region-of-interest-signaling (RoI-signaling) waveforms and high-frame-rate processing. This hybrid system is cost-effective, as discussed in subsequent sections of this paper. However, several challenges need to be overcome for developing new V2X communication technologies. These technical challenges and corresponding requirements are discussed in this paper.

The remainder of this paper is organized as follows. In Section II, we describe our OCC works and discuss general technical considerations of vehicular OWC/OCC systems.

A reference architecture of the vehicular OWC/OCC system using the hybrid waveform, i.e., hybrid-spatial-phase-shift-keying (HS-PSK), is then proposed. In Section III, we present technical considerations of the low-rate data stream. In addition, we provide details of the updated spatial-2-phase-shift-keying (S2-PSK) modulation scheme. In Section IV, we discuss technical considerations of the high-rate data stream and the proposed dimming-spatial-8-phase-shift-keying (DS8-PSK) single carrier for high-speed data transmission. In Section V, we analyze the performance of our modulation schemes based on the estimation of our proposed waveforms' bit error probability and an experiment for measuring the pixel signal-to-noise-ratio (SNR) using different types of cameras. Finally, in Section VI, we conclude the findings of the present work.

## II. PROPOSED VEHICULAR OWC/OCC SYSTEM

### A. TECHNICAL CONSIDERATIONS

Despite the potential of a lucrative market for automotive industry using OWC/OCC, it remains challenges for developing these new technologies. Several critical challenges must be considered for V2V/V2I using the visible light spectrum. Some of the typical challenges are discussed below.

The first challenge is the selection and initialization of interesting communication links from thousands of possible artificial lights. Therefore, an Rx camera should be able to detect and set up a communication link with an acceptable time delay. This means that many conventional solutions for object detection, which rely on computer vision, are not suitable for setting up OWC/OCC links due to the long time delay caused by their complex processes. In contrast, a smart camera can control its imaging parameters, e.g., frame rate and shutter speed, to detect RoI and set up a communication link to ensure better communication quality.

Another technical challenge is light source detection arising from the camera's ability. An Rx camera may not focus on all existing light sources simultaneously at different distances from its position due to the limitations of the imaging lens. This means that RoI detection depends on the feasibility of working with a very blurred image, in which not all light sources are focused by the camera.

The Rx cameras used in a vehicular OWC/OCC system should support both private and public communication modes. In detail, at the receiver side, whereas a car is communicating with its paired car in a private mode, other vehicles should be able to identify these two cars and receive a small dataset asynchronously to guarantee safety when moving on the same road.

Another challenge is that illumination, which is the primary purpose of light sources (vehicular, traffic, or signage lights), must be guaranteed with acceptable quality. Flicker-free illumination is one of the requirements with which any modulated light intensity must comply. Up to 200 Hz of optical modulation frequency can be considered as a safe range for human eyes [13]. Typical VLC physical layer (PHY) modes in IEEE 802.15.7-2011 are designed to operate at

optical clock rates higher than 10 kHz to provide flicker-free illumination, and this design is similar for OCC PHY modes. With such Tx optical clock rates, on the OCC receiver side, the sampling rate must adhere to the Nyquist sampling theorem. However, the frame rate parameters of many cameras cannot satisfy this sampling frequency. Thus, undersampling is considered as a solution to this problem.

In addition, high-resolution dimming may be necessary for specific scenarios. Currently, dimming support is one of the technical considerations in VLC/light fidelity (LiFi) specifications. Therefore, it is necessary that OWC/OCC systems support dimming.

The requirement of high-mobility support is critical for V2V/V2I communication. This is one of the most challenging tasks in vehicular OWC/OCC. The allowed speeds of vehicles under different conditions, which were surveyed in [2], are used to set the objectives of vehicular OWC/OCC systems.

The requirements of communication distance for different traffic conditions must also be considered. The required inter-vehicular distance for communication is up to 200m for highways or rural areas. An image of a light source may become a small point when the Tx is at a distance of 200m from the Rx. This is the minimum required inter-vehicular distance. Thus, OWC/OCC systems must support this nearly point communication protocol.

The proposed technologies must be compatible with a variety of hardware available on the market. This last consideration is mentioned in relation to the feasibility of commercialization, not in relation to technical feasibility. Currently, two types of cameras are available on the market, i.e., rolling shutter and global shutter. An OWC/OCC waveform should be designed to support either type of camera or both types of cameras. Moreover, such an OWC/OCC waveform should be implemented using a wide range of Tx light sources with varying parameters, including size, shape, and illumination characteristics.

## B. OUR MAJOR CONTRIBUTIONS

In the present paper, we present our contributions to V2X communication. The first contribution is the proposed hybrid waveform HS-PSK with a novel DS8-PSK waveform for high-rate data streams. To evaluate the applicability of the HS-PSK waveform to V2X communication, SNR measurement experiments were conducted using a vehicular lighting model and various types of cameras. The experimental results aim to confirm the technical feasibility of the proposed vehicular communication system employing a hybrid waveform.

After the release of the IEEE 802.15.7-2011 standard [14], it was found that nonspecific V2V or V2I regulation is provided [2]. This standard has been modified by the Task Group 7m (TG7m). The PHY IV mode, which was introduced in the IEEE 802.15.7-2018 standard, is intended for vehicular applications. The RoI-signaling technique for OCC has recently been introduced into the PHY IV mode. Intel and Kookmin University have proposed and contributed to the RoI technique of the TG7m during meetings. A proposal

from Intel has been at the forefront of this RoI implementation. Their undersampled frequency shift on-off keying (UFSOOK) is capable of delivering the short identities of multiple-input multiple-output (MIMO) light sources [15]. The spatial-2-phase-shift-keying (S2-PSK) scheme that we proposed [11] aims to support vehicles in terms of tracking/identifying MIMO light sources. These two RoI-signaling modulation schemes are addressed in the PHY IV mode of the IEEE 802.15.7-2018 standard. The modulation scheme in the PHY IV mode should support the detection and tracking of numerous light sources with communication data in a manner compatible with various types of low-frame-rate cameras, should be flicker-free, and should make communication possible over large distances among a copious amount of noisy light sources on the road.

The next generation of OCC systems with both adaptive-RoI detection and high-rate data transmission ability has novel features to deploy. A vehicular OWC/OCC system using a hybrid waveform that consists of low-rate and high-rate data streams can mitigate the computational load on the receiver, thus, reducing the processing time. Our proposed HS-PSK single carrier is such a hybrid waveform. HS-PSK, which we first introduced in [16], is a combination of a low-rate S2-PSK waveform and a high-rate DS8-PSK waveform. The S2-PSK data stream is generated based on changes between the low and high dimming levels of the DS8-PSK waveform. The novel contributions of the proposed hybrid high-rate waveform DS8-PSK that can be transmitted over selectable RoI links are summarized as follows:

- High-resolution dimming. The two dimming levels of the proposed high-rate waveform generate two binary states of the RoI-signaling waveform. However, at each dimming level, a high-quality light intensity must be maintained. This newly designed waveform can support dimming in steps of 12.5% without affecting communication performance.
- Intelligent decoding ability to decrease the frame rate requirement. Undeniably, a camera cannot decode data if the LED states are fuzzy. The proposed waveform can support the decoding process based on fuzzy states of LEDs. Therefore, this concept can help to reduce the frame rate requirement of the camera at least twice times compared with that in the binary-based decoding method.

In addition to theoretical estimation of the SNR of the low-rate data stream, we conducted SNR measurement experiments with rolling shutter and global shutter cameras to validate the technical feasibility of optical V2X communication by using the proposed hybrid waveform (HS-PSK). In these two experiments, SNR measurements were recorded using different exposure time settings and distances in daytime, wherein background light noise always exists, to demonstrate that a low-power LED can be used for transmission over a distance of approximately 50m. The experimental results show that a real vehicular headlight or tail light with power

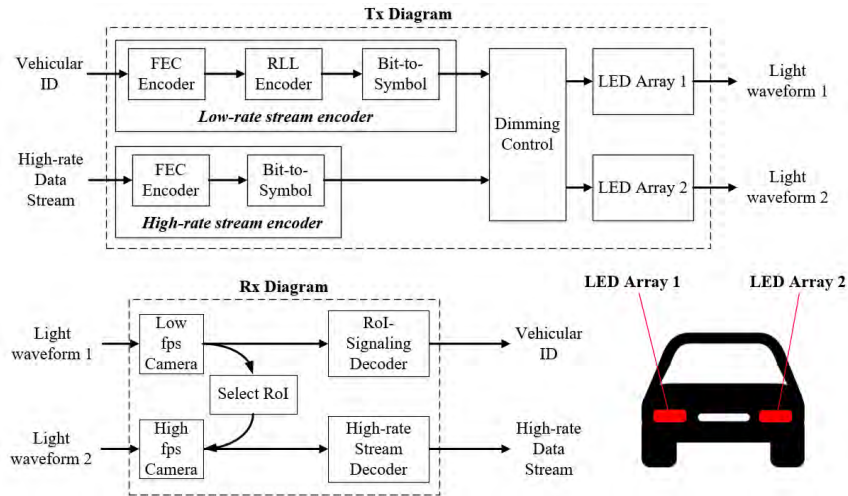


FIGURE 1. Block diagram of the reference architecture of a typical HS-PSK system.

around 20 times higher than that of a low-power LED can support communication over distances of up to 200m. This distance is one of the technical requirements of vehicular communication systems, as mentioned in Section II(A).

### C. REFERENCE ARCHITECTURE

In this subsection, we present the technical details of the HS-PSK system. As discussed earlier, visible light intensity modulation rate, which has a frequency of up to 200 Hz, is safe for human eyes. Thus, the optical clock rate of OCC modulation schemes should be designed to operate at more than this safe frequency threshold. According to the Nyquist theorem, at the receiver side, the camera's frame rate must be at least double the modulation rate to achieve proper sampling. The oversampling technique should be implemented in this scenario, where the camera sampling rate (i.e., frame rate) is higher than the optical clock rate. Thus, this technique requires a high-speed camera. However, when a high-speed camera is implemented in the Rx side, the maintenance of the high-speed frame rate while handling heavy processing involved in Tx light source detection and data demodulation increases the computational workload in the Rx. Therefore, this scenario is cost-ineffective. Consequently, the incorporation of the RoI-signaling waveform and the high-rate data stream in vehicular OCC system is proposed to mitigate the processing workload of the Rx and minimize the computational cost in light source detection and extraction of the system.

The overall architecture of the proposed system is shown in FIGURE 1. The low-rate and high-rate data streams can be transmitted using the LED arrays (LED headlights, LED tail lights, etc.) of vehicles. The proposed S2-PSK can be a candidate for a low-rate RoI-signaling scheme, whereas DS8-PSK can be modulated as the high-rate data stream. The high-rate data stream is embedded into the low-rate RoI stream. Dual streaming of light source identification

signaling and high-speed data link is performed as the hybrid modulation.

In the Rx side, the low-frame-rate camera initially detects and selects the RoI of the light source to extract data from the low-rate data stream. The transmission of RoI is beneficial when the Rx camera knows the area where the communication link must be set up. The Tx light source shall continuously inform the Rx camera via a known signal to distinguish between the Tx light source and other noninterested light sources or objects. The high-frame-rate camera can be activated to receive high-speed data stream via the detected RoI, which contains the information needed to assist safe driving.

### D. HS-PSK HYBRID WAVEFORM

FIGURE 2 shows the formation of an HS-PSK hybrid waveform. HS-PSK and Twinkle-VPPM [17], introduced by Intel, are two hybrid modulation schemes addressed in the PHY IV mode of the IEEE 802.15.7-2018 standard, which are intended to be applied in the optical communication system. Twinkle-VPPM is the combination of UFSOOK for modulating a low-rate data stream and VPPM for a high-rate data stream, whereas HS-PSK is a combination of a low-rate S2-PSK waveform and a high-rate DS8-PSK waveform.

In HS-PSK, the S2-PSK data stream is generated based on changes between low and high dimming levels of the DS8-PSK waveform. The S2-PSK modulator controls changes in dimming levels during DS8-PSK encoding and, therefore, generates S2-PSK low-rate waveform as an amplitude modulation (AM) signal at a low frequency. It means that the S2-PSK clock interval is higher than the DS8-PSK clock interval.

For an Rx system with dual cameras, the S2-PSK waveform is decoded by a rolling shutter camera or a global shutter camera with a low frame rate (e.g., 30 fps), whereas the high-rate DS8-PSK waveform is decoded by a high-speed global shutter camera (e.g., 1 kfps). An Rx camera with

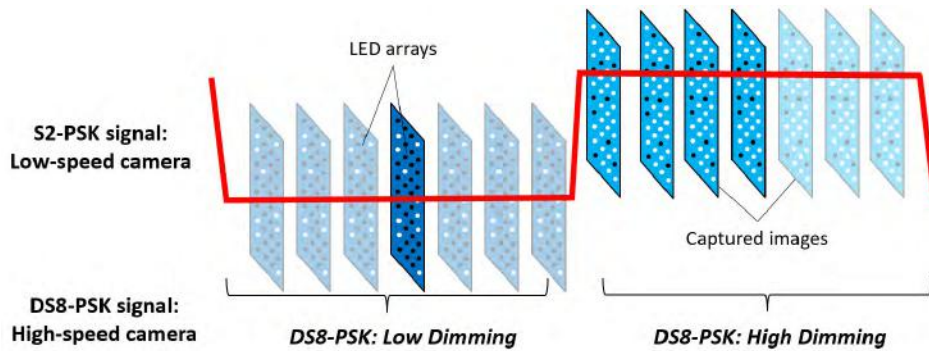


FIGURE 2. Illustration of a hybrid waveform using S2-PSK and DS8-PSK modulation schemes.

slow exposure time can only see the dimming levels of all LEDs in the same image, whereas an Rx camera with fast exposure time can clearly see the amplitude of each LED in a LED array. The amplitude of the S2-PSK waveform can be calculated from the average dimming level of the transmitter. The operations of the S2-PSK modulator and the high-rate DS8-PSK modulator are described in Section III and Section IV, respectively.

### III. LOW-RATE MODULATION SCHEMES

#### A. LOW-RATE DATA STREAM REQUIREMENTS

The development of RoI-signaling waveforms was inspired by the shortcomings of conventional computer vision (CV) for light source detection. A comparison of the features of RoI-signaling waveforms and CV-based concepts are summarized as follows:

- The object detection ability of CV-based solutions typically relies on the analysis of pattern images. Therefore, this method incurs high computational workload. Moreover, the light intensity from light source objects detected by receivers does not provide information to Rx vehicles. In contrast, RoI-signaling waveforms, which are transmitted by light sources, are informative for Rx to process.
- The performance of CV-based object detection is poor when the input images are blurry. By analyzing pixel-based modulated waveforms, it is possible to detect and track light sources of interest, even when only the pixel intensity of the light source on the image is perceptible.
- The computational complexity of image processing using conventional CV-based solutions limits the processing frame rate of the Rx. CV uses two-dimensional image processing, whereas the RoI-signaling technique uses one-dimensional binary sequence processing. Moreover, the RoI-signaling decoder may focus only on processing the temporal sequence of pixel intensity of light sources, which is a very small part of an image sequence. Consequently, the proposed RoI-signaling technique may considerably reduce the image processing time compared with CV, resulting in

a high frame rate in the light-source-tracking process of RoI-signaling.

Undeniably, pixel-based modulated waveforms can be used to detect the desired informative light sources among copious amount of artificial light sources encountered by vehicular OCC systems. Although the RoI-signaling technique has potential advantages over the CV-based method, many challenges are encountered in designing RoI-signaling waveforms, as discussed below:

- The capability to support a large range of multi-LED arrays in the market. This concern pertains to commercialization. Conceptually, each LED array on the same light source is required to bring the same information modulated by the RoI-signaling waveform for the Rx to be able to identify them.
- Flicker-free is a mandatory requirement for visible light usage on vehicles. As previously mentioned, illumination is the most important purpose of the lighting system on vehicles. Therefore, the quality and safety of light intensity to human eyes must be considered. However, the safe frequency threshold for human eyes is considerably higher than a typical camera's frame rate. Therefore, the use of undersampling is proposed as a solution for the RoI-signaling waveform.
- The ability to guarantee acceptable RoI-signaling demodulation performance under dimming. In a few specific scenarios, light sources must be operated in dimming modes. Therefore, the proposed RoI-signaling modulation schemes must be able to adapt to different dimming levels.
- The sampling method for the RoI-signaling waveform should support different types of camera shutter mechanisms. Different shutter mechanisms require different approaches for the Rx camera, even when the same modulation scheme is deployed. Cameras with two different types of shutters are commercially available, i.e., rolling and global. Therefore, support for the RoI-signaling waveform from only rolling shutter cameras, only global shutter cameras, or both should be considered to ensure commercial effectiveness.

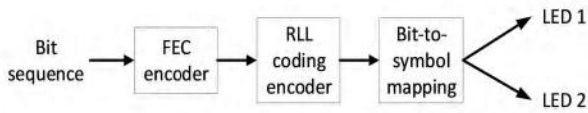


FIGURE 3. Reference architecture of an S2-PSK transmitter.

- The ability to support mobility conditions for vehicles during communication. The proposed low-rate data stream should be able to support vehicles in various circumstances, such as fast-moving conditions and sampling errors due to camera rotation.

**B. S2-PSK ENCODING**

A reference architecture of an S2-PSK transmitter is shown in FIGURE 3.

A modulation scheme closely related to S2-PSK, called undersampled-phase-shift-on-off-keying (UPSOOK), was introduced by Luo et al. [18] in 2014. It generates an under-sampled waveform for one light source based on two phase-shift-keying. Notably, the proposed S2-PSK is developed for vehicles, which always have pairs of lights. In this modulation scheme, the S2-PSK transmitter transmits data by controlling the phase relationship between the two waveforms generated by a pair of light sources. This means that when bit “1” is transmitted through two inversed phase waveforms, bit “0” is transmitted through waveforms with the two same-phase waveforms. The waveform of the first LED source during a cycle  $T$  is expressed by Equation (1).

$$s_1(t_k) = \begin{cases} 1, & 0 \leq t_k < T/2 \\ 0, & T/2 \leq t_k < T \end{cases} \quad (1)$$

The full waveform of the first LED source is expressed by Equation (2). The interval of a bit ( $T_{bit}$ ), which is used to guarantee the flicker-free condition, is higher than the waveform cycle ( $T$ ) (i.e.,  $T_{bit} = NT$ ).

$$s_1(t) = \sum_{k=0}^N s_1(t_k + kT) \quad (2)$$

where  $\begin{cases} 0 \leq t < T_{bit} \\ s_1(t_k + kT) = s_1(t_k) \end{cases}$

The full waveform of the second LED source is expressed by Equation (3), where  $s_2(t_k)$  is the cycle  $k$  among  $N$  cycles and  $s_1(t_k)$  is the inverse form of  $s_1(t_k)$ .

$$s_2(t) = \sum_{k=0}^N s_2(t_k + kT) \quad (3)$$

where  $\begin{cases} 0 \leq t < T_{bit} \\ s_2(t_k) = \begin{cases} s_1(t_k) & \text{if } (bit = 0) \\ \bar{s}_1(t_k) & \text{if } (bit = 1) \end{cases} \end{cases}$

The modulation clock rate is set to a fixed value. However, the frame rate of the receiver is customized by changing the

TABLE 1. S2-PSK line coding.

Bit input	Code output
0	00
1	01

bit interval ( $T_{bit}$ ). For example, a 200 Hz clock rate with  $N = 20$  can provide a 10 bps link that can support a low-frame-rate camera at 20 fps. The proposed run-length limited (RLL) coding at the 1/2-code rate, as introduced in TABLE 1, is not only a general RLL coding that provides DC balance but is also used for correcting sampling error caused by time deviations between two light sources.

**C. S2-PSK DECODING METHOD**

1) SPATIAL-XOR MODEL

To decode an S2-PSK signal, the bit value is decided using the spatial-XOR model from an image of two LEDs. This method represents a typical class of S2-PSK decoding algorithms. The output bit is “0” if the captured states of two LED waveforms are in the same phase, whereas the output bit is “1” for other captured states.

2) CROSS-CHECK-XOR MODEL

In the sampling process, if the Rx uses a global shutter camera, two LEDs on the Tx are captured simultaneously. Therefore, it is easier to decode the data from the Tx by using the spatial-XOR model. However, in practice, if the Rx employs a rolling shutter camera, the rotation problem must be considered. Different sampling times on the same image due to the rolling shutter camera can introduce errors into the spatial-XOR operation. In this circumstance, RLL coding can be applied to avoid sampling error. By applying RLL coding to the transmitted signal, the received bit remains correct even if two RLL binaries belonging to a bit are affected. Nevertheless, the error occurs if one of the two RLL binaries is affected. Therefore, we propose a cross-check-XOR model to overcome this sampling error problem.

When there is a rotation problem, we assume that the rotation angle of the camera does not change in two adjacent images for decoding. Under this assumption, the sampling time difference between two LEDs remains the same for two adjacent images. The sampling time deviation caused by rotation can be calculated using Equation (4):

$$\Delta t = N_{pixel} \times \frac{1}{F_s} \quad (4)$$

where  $N_{pixel}$  is the number of different pixel rows between two light sources captured in the same image and  $F_s$  is the sampling rate of the rolling shutter camera.

The assumption of constant deviation in sampling time holds under the condition that LEDs move vertically or horizontally between images. However, if the rotation angles of the camera are different for two images, the sampling time deviation may change, leading to errors. In this case, forward

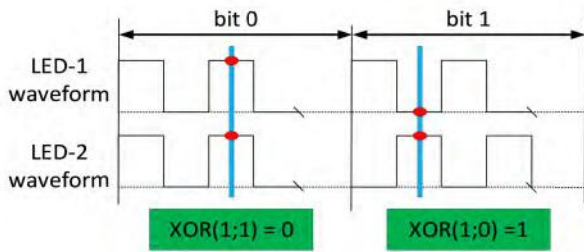


FIGURE 4. Example of decoding S2-PSK using the spatial-XOR.

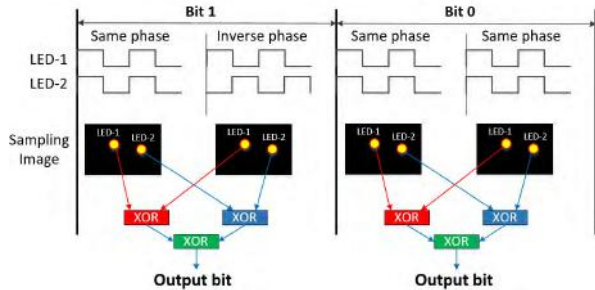


FIGURE 5. Illustration of decoding a bit from two adjacent images.

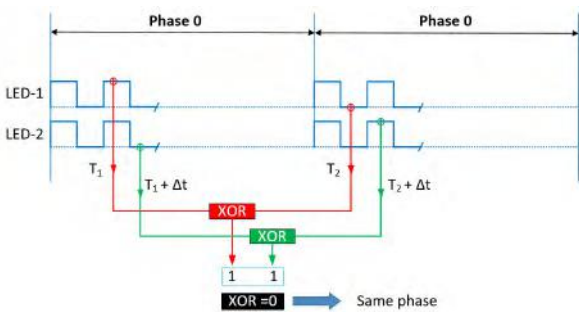


FIGURE 6. Decoding output when LEDs transmit same phases.

error correction (FEC) may be applied to correct the sampling errors. Another assumption is that each phase interval can be captured in an image by setting the camera's frame rate equal to the phase interval. Thereafter, a data bit can be decoded by using a cross-check algorithm from two adjacent images, as shown in FIGURE 5. The sampling time deviation is unknown due to random sampling time and variation in the camera's frame rate. Even so, the output of the cross-check XOR model is accurate, similar to the examples shown in FIGURE 6 and FIGURE 7.

#### IV. HIGH-RATE DATA STREAM VIA SELECTED ROI

##### A. HIGH-RATE DATA STREAM REQUIREMENTS

Dimming support is mandatory and is the first thing to consider for high-rate data streams. The optical clock rate of high-rate modulation schemes must be synchronized with the optical clock rate of low-rate RoI-signaling schemes. Meanwhile, a high-rate data stream must maintain acceptable performance under dimming when integrated with a low-rate data stream by dimming.

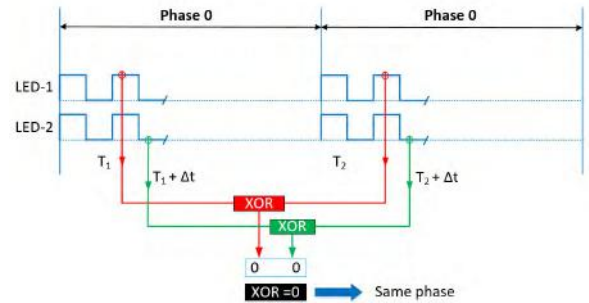


FIGURE 7. Decoding output when LEDs transmit inverse phases.

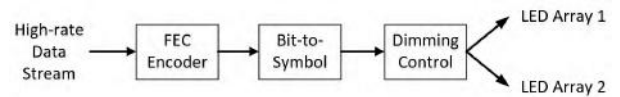


FIGURE 8. A reference architecture of a DS8-PSK transmitter.

The second technical consideration is that the sampling rate of the high-frame-rate camera must follow the Nyquist theorem to achieve the correct high-rate waveform. A mega-frame-per-second (Mfps) camera is currently available on the market. However, this study aims to find alternatives that are cost-effective. High-rate modulation schemes can be decoded by cameras with frame rates of less than 20 kilo-frame-per-second (kfps). Thus, to achieve high data rate without increasing the camera's frame rate, applying multi-LED arrays is considered as a solution.

##### B. HS-PSK WAVEFORM

HS-PSK is a type of single-carrier waveform that can be used to modulate and transmit low-rate and high-rate data streams. It is a combination of S2-PSK and DS8-PSK. The HS-PSK waveform can be transmitted using a pair of light sources on a vehicle. DS8-PSK controls the pulse-width dimming level to generate the low-rate S2-PSK waveform. This modulation scheme has been added to the new IEEE 802.15.7-2018 standard.

##### 1) DS8-PSK MODULATOR

A reference architecture of a DS8-PSK transmitter is shown in FIGURE 8. The DS8-PSK waveform is transmitted using a pair of light sources, which comprises a reference LED group and a data LED group. Clusters of three bits from the input high-rate data stream are modulated based on the phase-shift value between two transmitted waveforms, which are driven by a pair of light sources. To support the mapping of the clusters of three bits of an input bit string into a phase-shift value, the DS8-PSK duty cycle must be separated into eight time slots. In addition, the number of LEDs in each light source should be eight. The waveform generated by each LED in a light source is a square wave. Within a light source, the  $(i+1)^{th}$  waveform is delayed by  $1/8$  duty cycle compared with the  $i^{th}$  waveform.

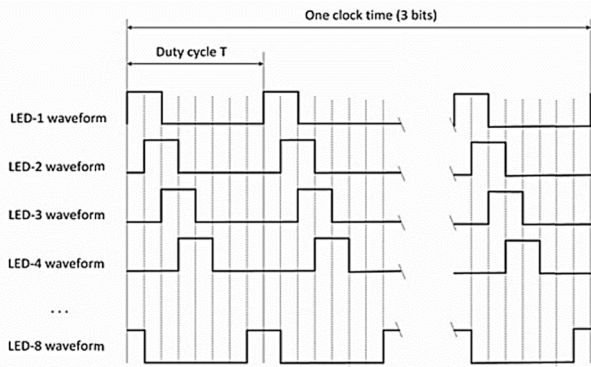


FIGURE 9. Example of a DS8-PSK waveform of a LED group with 25% (2/8) dimming level.

TABLE 2. Mapping table from bits to  $S_{Phase\_Shift}$ .

3 bits input	$S_{Phase\_Shift}/(T/8)$ output
000	0
001	1
010	2
011	3
100	4
101	5
110	6
111	7

When transmitting Tx data, all phases of the waveforms, which are generated by the reference LED group, are maintained from 0,  $T/8$ , and up to  $7T/8$ , whereas all phases of the waveforms generated by the data LED group are shifted as compared with the waveforms in the first LED group based on the phase-shift value. The phase-shift value of a pair of light sources is called  $S_{Phase\_Shift}$ . It can be calculated using Equation (5) by considering the value of  $i$ , where  $T$  is the duty cycle of a LED waveform. The mapping of three bits onto the  $S_{Phase\_Shift}$  value by considering the value of  $i$  is shown in TABLE 2.

$$S_{Phase\_Shift} = i \times \frac{T}{8} \tag{5}$$

DS8-PSK supports dimming in steps of  $1/8$  (12.5%) of a duty cycle  $T$ . The dimming level can be calculated by the sum of “1” state among eight time slots in a duty cycle  $T$  as expressed by Equation (6). Thus, the DS8-PSK waveform can support seven dimming levels from  $1/8$  (12.5%),  $2/8$  (25%), and up to  $7/8$  (87.5%). FIGURE 9 shows the DS8-PSK waveform of a LED group with 25% dimming level. The data rate of each LED group is calculated using Equation (7). For example, with an optical clock rate and a symbol rate of 10 kHz and 10 symbols/sec, respectively, the transmission data rate achieved by a data LED group is 30 bps.

$$Dimming\_level = \left( \sum 'State\_1' \right) / 8 \tag{6}$$

$$Data\_rate(bps) = (bit/symbol) \times (symbol\_rate) \tag{7}$$

## 2) DS8-PSK DECODER

At a given sampling time, the Rx camera simultaneously captures two groups of light sources in an image. Each LED group in an image will form a discrete waveform, comprising eight “1” or “0” states. Each set of states is called  $S_{Phase}$ . Based on the dimming levels supported by DS8-PSK, seven tables can be formed for decoding at seven corresponding dimming levels. In the first step of decoding a DS8-PSK waveform, the  $S_{Phase}$  value should be selected from the proper  $S_{Phase}$  decoding table, as presented in TABLE 3. Then, the spatial phase value ( $S_{Phase\_Shift}$ ) can be calculated based on the  $S_{Phase}$  value of the reference LED group and the  $S_{Phase}$  value of the data LED group. Equation (8) shows how to calculate the  $S_{Phase\_Shift}$  value, while FIGURE 10 shows an example of how to determine  $S_{Phase\_Shift}$ . When the  $S_{Phase\_Shift}$  value is detected, the data bits can be decoded inversely by using the mapping table presented in TABLE 2.

$$S_{Phase\_Shift} = S_{Phase}(data) - S_{Phase}(reference) \tag{8}$$

At any given sampling time, the Rx camera may capture an unclear state of a LED waveform, which is called bad sampling. Obtaining fuzzy states is unavoidable in the sampling process. This may happen when the Rx camera captures an image at the transition time of the waveform of a single LED. In a conventional decoder, the camera’s frame rate must be higher than the transmitted optical clock rate to avoid fuzzy states during sampling. However, by proposing a novel de-mapping table, as shown in TABLE 4, unclear states can be mitigated. FIGURE 11 illustrates the sampling times in which good sampling or bad sampling may occur. However, at the time of sampling, owing to the proposed phase-shifted waveform of each LED in a group, only one or no bad sampling occurs. Therefore, it is easy to detect and mitigate the sampling error.

At the time corresponding to bad sampling, the  $S_{Phase}$  value can be determined from TABLE 4, which includes sets of LED group states with unclear states. By contrast, owing to the complexity of the operational environment, a neural network (NN) classification can be implemented in the DS8-PSK decoder to mitigate the bad sampling problem. This is in addition to the decoding method for fuzzy states by looking up a table of unclear states. The application of the NN to the DS8-PSK decoder makes the process easy and effective for users without requiring deep mathematical knowledge. A suitable NN model and a training dataset based on a decoding table are required to correctly classify the LED states.

## C. VPPM WAVEFORM

The VPPM modulation scheme is implemented in the IEEE 802.5.7-2011 standard. It uses binary pulse-position modulation (PPM) for communication and the pulse width for dimming control. Bit “0” is when the pulse is aligned to the left of the symbol period, whereas bit “1” is when

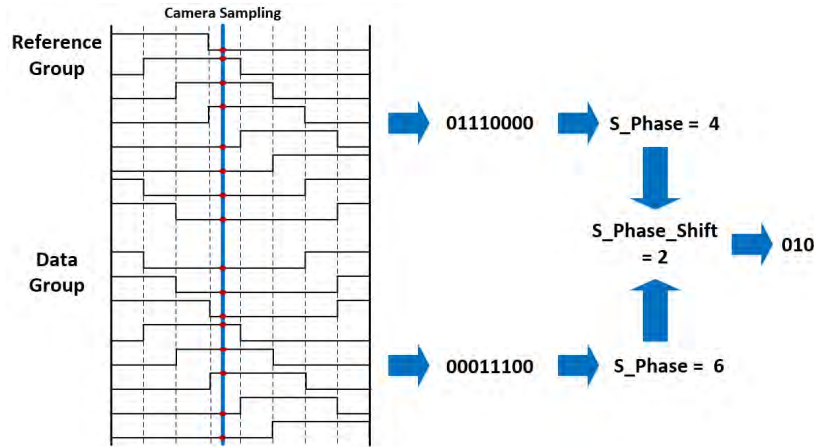


FIGURE 10. Illustration of sampling a DS8-PSK waveform and calculating  $S\_Phase\_Shift$ .

TABLE 3.  $S\_Phase$  values and captured set of LED group states under various dimming conditions.

8 states input							$S\_Phase$ output
Dimming 1/8	Dimming 2/8	Dimming 3/8	Dimming 4/8	Dimming 5/8	Dimming 6/8	Dimming 7/8	
1000 0000	1000 0001	1000 0011	1000 0111	1000 1111	1001 1111	1011 1111	1
0100 0000	1100 0000	1100 0001	1100 0011	1100 0111	1100 1111	1101 1111	2
0010 0000	0110 0000	1110 0000	1110 0001	1110 0011	1110 0111	1110 1111	3
0001 0000	0011 0000	0111 0000	1111 0000	1111 0001	1111 0011	1111 0111	4
0000 1000	0001 1000	0011 1000	0111 1000	1111 1000	1111 1001	1111 1011	5
0000 0100	0000 1100	0001 1100	0011 1100	0111 1100	1111 1100	1111 1101	6
0000 0010	0000 0110	0000 1110	0001 1110	0011 1110	0111 1110	1111 1110	7
0000 0001	0000 0011	0000 0111	0000 1111	0001 1111	0011 1111	0111 1111	8

the pulse is aligned to the right of the symbol period. Various pulse-width levels generate VPPM waveforms with various dimming levels. The VPPM signal is expressed by Equation (9) [19].

$$s(t) = \begin{cases} \sqrt{E_s \times \frac{d}{50}} \times \varphi_0(t), & b = 0 \\ \sqrt{E_s \times \frac{d}{50}} \times \varphi_1(t) & b = 1 \end{cases} \quad (9)$$

where  $E_s$  is the symbol energy,  $d$  is the dimming level ( $0 \leq d \leq 100$ ), and  $\varphi_i(t)$  is the basic function, which is changed according to the dimming level and defined by Equation (10).

$$\varphi_0(t) = \begin{cases} \sqrt{\frac{100}{d \times T}}, & 0 \leq t \leq \frac{d \times T}{100} \\ 0, & \text{otherwise} \end{cases}$$

$$\varphi_1(t) = \begin{cases} \sqrt{\frac{100}{d \times T}}, & \left(1 - \frac{d}{100}\right) \times T \leq t \leq T \\ 0, & \text{otherwise} \end{cases} \quad (10)$$

VPPM can be combined with another low-rate modulation scheme to produce a hybrid waveform. The VPPM proposed by Intel is an example of such a hybrid waveform.

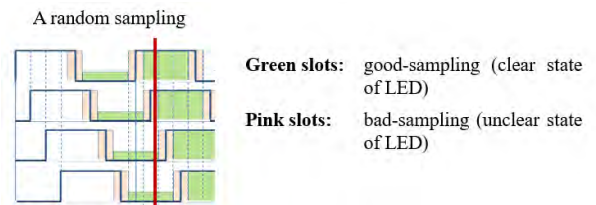


FIGURE 11. Illustration of good sampling and bad sampling at the sampling moment.

UFSOOK transmits vehicular identity as an RoI-signaling waveform, whereas rapid changes in the VPPM clock rate generate the high-rate data stream. Pulse-width control plays an important role not only in supporting various dimming levels of the light source but also in generating a low-frequency AM signal that can be decoded as a low-rate data stream by using a low-frame-rate camera. At a given sampling time, whereas a high-speed Rx camera decodes the high-rate data stream, another Rx camera with slow exposure time (e.g., 30 fps) can be used to receive an optical signal of constant intensity. Therefore, the low-frame-rate Rx camera can only gather the samples required to create the low-rate data stream.

TABLE 4. S\_Phase values and captured set of LED group states with unclear states under various dimming conditions.

8 states input							S_Phase output
Dimming 1/8	Dimming 2/8	Dimming 3/8	Dimming 4/8	Dimming 5/8	Dimming 6/8	Dimming 7/8	
xx00 0000	1x00 000x	1x00 00x1	1x00 0x11	1000 1111	1x0x 1111	1xx1 1111	1
0xx0 0000	x1x0 0000	11x0 000x	11x0 00x1	1100 0111	11x0 x111	11xx 1111	2
00xx 0000	0x1x 0000	x11x 0000	111x 000x	1110 0011	111x 0x11	111x x111	3
000x x000	00x1 x000	0x11 x000	x111 x000	1111 0001	1111 x0x1	1111 xx11	4
0000 xx00	000x 1x00	00x1 1x00	0x11 1x00	1111 1000	1111 1x0x	1111 1xx1	5
0000 0xx0	0000 x1x0	000x 11x0	00x1 11x0	0111 1100	x111 11x0	1111 11xx	6
0000 00xx	0000 0x1x	0000 x11x	000x 111x	0011 1110	0x11 111x	x111 111x	7
x000 000x	x000 00x1	x000 0x11	x000 x111	x00x 1111	x0x1 1111	xx11 1111	8

V. PERFORMANCE EVALUATION AND EXPERIMENTAL VALIDATION

A. LOW-RATE ROI-SIGNALING MODE

1) PIXEL  $E_b/N_0$  COMPUTATION AND NOISE MODELING

Pixel noise in charge-coupled-device/complementary-metal-oxide-semiconductor (CCD/CMOS) cameras can be approximately modeled by Equation (11) [17].

$$n \sim N(0, \sigma(s)^2) \tag{11}$$

where  $s$  is the pixel value,  $\sigma^2(s) = s.a.\alpha + \beta$  with  $a$  representing the mark and space amplitude, and  $\alpha$  and  $\beta$  are the fitting parameters obtained from experiments. Here, we used the values  $\alpha = 0.01529$  and  $\beta = 0.1973$ , which were estimated experimentally from [17]. The pixel SNR (or  $E_b/N_0$ ) of an Rx camera can be estimated by Equation (12) with the assumption that one symbol contains one bit.

$$Pixel \frac{E_b}{N_0} = \frac{E[s^2]}{E[n^2]} \approx \frac{a^2.\Delta}{a.\alpha.\Delta + \beta} \tag{12}$$

where  $E_b$  is the bit energy,  $N_0$  is the noise density,  $s$  is the pixel value,  $a$  is the mark and space amplitude,  $\Delta = T_{exposure}/T_{bit}$  is the ratio of the camera’s exposure time and bit interval, and  $\alpha$  and  $\beta$  are the fitting parameters.

This estimation should be done for each camera because a standard does not exist for all camera parameters. Using Equation (12), an example of a theoretical estimation of pixel SNR for a chosen camera with a shutter speed of 10 kHz and an optical clock rate transmitter of 1 kHz is shown in FIGURE 12, which shows a nonlinear curve. Even when no Tx signal is transmitted, noise still exists. When the S2-PSK signal samples reach the maximum pixel amplitude of the 8-bit ADC in the Rx camera, a high value of pixel SNR (approximately 40 dB) can be achieved. Pixel SNR can be used to approximate the bit error probability. Therefore, this relationship is very useful in practice for estimating a system’s pixel SNR by measuring pixel amplitude values.

2) SNR MEASUREMENT FOR VEHICULAR OCC

Our previous paper [3] analyzed the performance of some undersampled single-carrier modulation schemes in OCC,

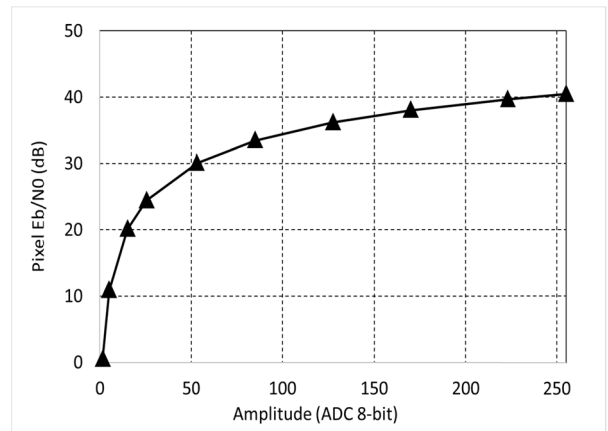


FIGURE 12. Theoretical calculation of the relationship between pixel SNR and BER.

such as UPSOOK or UFSOOK. We found single-carrier modulation schemes, such as S2-PSK, require at least 10 dB to achieve a bit error rate (BER) of  $10^{-4}$ . Practical pixel SNR measurements were performed to confirm the pixel SNR satisfaction for the desired BER value, such as  $10^{-4}$ . Both the rolling shutter and global shutter cameras were used to measure pixel SNR levels at different distances. In the first experiment, a board with 12 VDC – 2.5 W LEDs measuring 3 cm in diameter was used as a model of vehicular tail lights. The device setup used in the first experiment is shown in FIGURE 13 to FIGURE 16. Pixel SNR was measured based on changes in distances and exposure time values. A Point-Grey rolling shutter camera and a National Instruments global shutter camera can support exposure times as short as 50  $\mu s$  or even 33  $\mu s$ . The National Instruments global shutter camera was used to conduct measurements in daytime with ambient lights. Pixel SNR values were recorded at distances of 5–20m with specific exposure values of 33–500  $\mu s$ . The pixel SNR measurement results of the first experiment are shown in FIGURE 17 to FIGURE 20.

FIGURE 17 and FIGURE 18 show the amplitude values of light intensity sampled by the rolling shutter camera and the global shutter camera, respectively. The light intensities of the LEDs were sampled when the LED was ON (blue line)

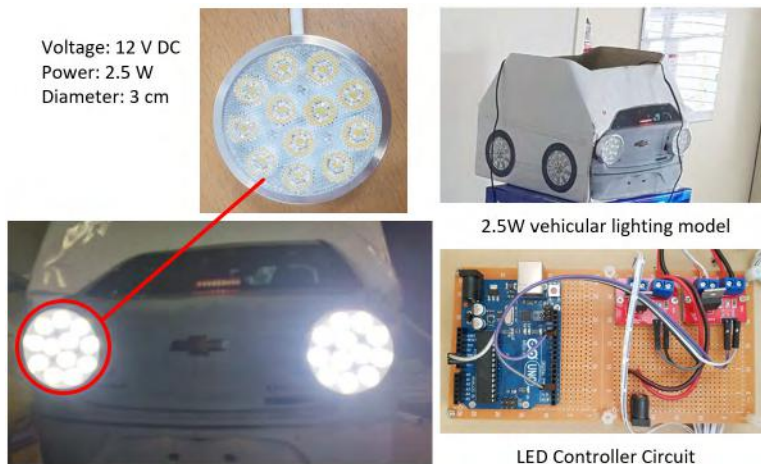


FIGURE 13. A 2.5 W vehicular lighting model for pixel SNR measurement experiments.

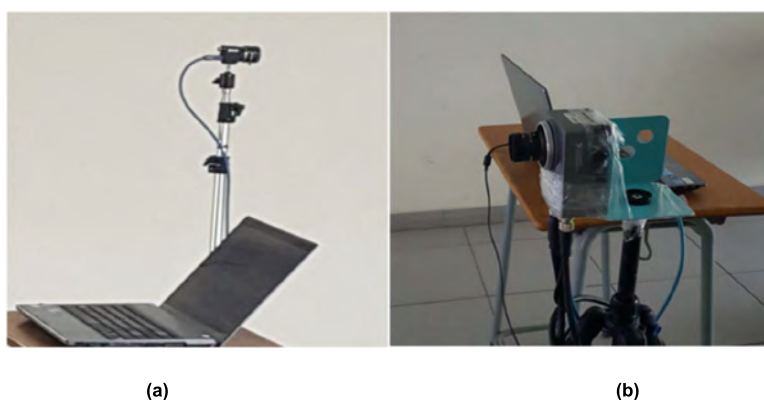


FIGURE 14. Cameras used for SNR measurement. (a) PointGrey rolling shutter camera. (b) National Instrument global shutter camera.

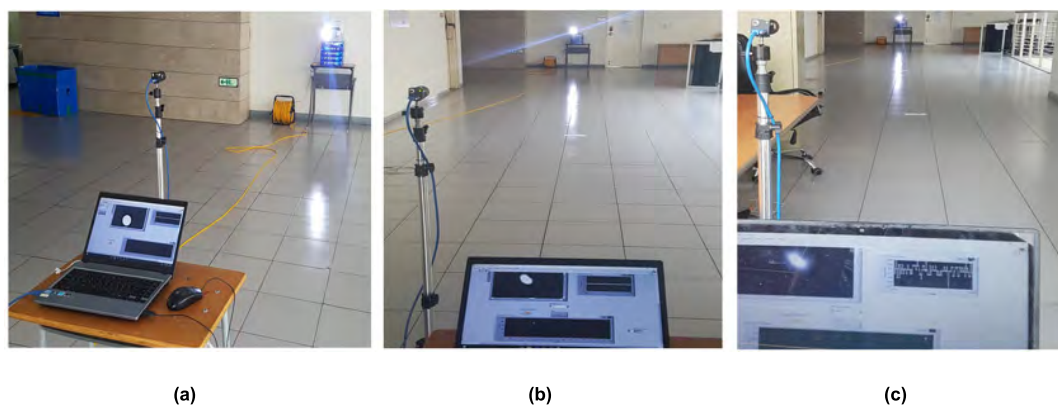


FIGURE 15. SNR measurement using a rolling shutter camera at different distances: (a) 5m, (b) 15m, and (c) 20m.

and OFF (red line). The measurement result of pixel SNR using a rolling shutter camera is shown in FIGURE 19(a). The corresponding fitting curve in FIGURE 19(b) provides a comprehensive insight into the relationship between pixel SNR and adaptive exposure control. The measurement

result of pixel SNR using a global shutter camera is shown in 20(a), and the corresponding fitting curve is shown in 20(b).

A second SNR measurement experiment using either a rolling shutter camera or a global shutter camera was

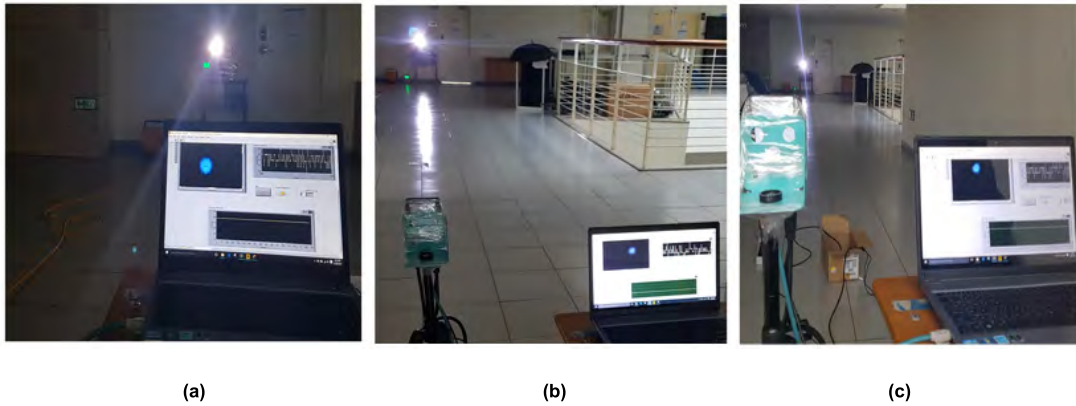


FIGURE 16. SNR measurement using a global shutter camera at different distances: (a) 5m, (b) 15m, and (c) 20m.

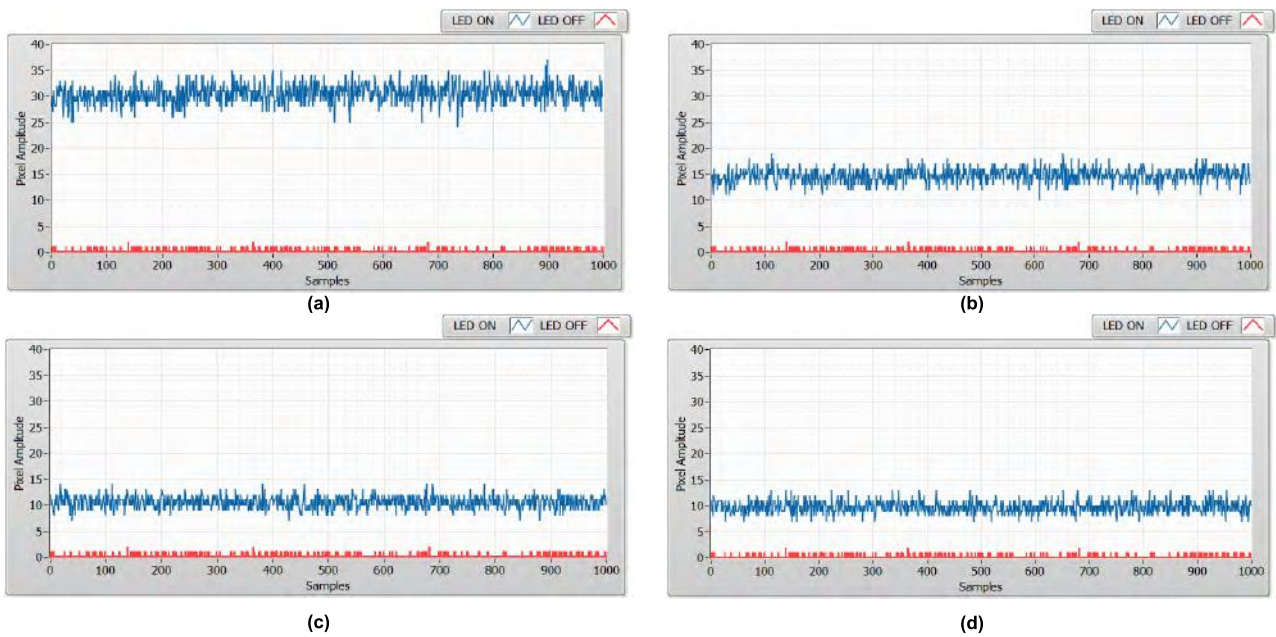


FIGURE 17. Pixel amplitude sampling results at 50  $\mu$ s exposure time setting using a rolling shutter camera at different distances: (a) 5m, (b) 10m, (c) 15m, and (d) 20m.

conducted using a bigger vehicular lighting model with 12 VDC – 30 W LED array to guarantee the ability to use OCC at a distance of 200m. The power of this vehicular lighting model is similar to a real light source in a car, whereas the 200m distance is a minimum requirement for inter-vehicular communication in highways or rural areas, as discussed in Section II(A). This second experiment was also performed in daytime. Similar to the first experiment with a 2.5 W vehicular lighting model, cameras with 16mm focal length were configured in different exposure time values to measure the SNR level of the light source. Pixel SNR values were recorded at distances of 50–200m with specific exposure values of 33–500  $\mu$ s. A 30 W vehicular lighting model and the device setup used in this second experiment are shown in FIGURE 21(a) and FIGURE 21(b), respectively. Measurement results of SNR and fitting curves for a rolling

shutter camera and a global shutter camera are shown in FIGURE 22 and FIGURE 23, respectively.

Note that exposure time significantly influences pixel SNR (or  $E_b/N_o$ ). A camera can be considered as a low-pass filter with long exposure time attenuating high-tone signals. Hence, a high pixel SNR can be achieved by setting a long exposure time. The total noise power spread over the occupied bandwidth can be reduced, leading to decreased communication bandwidth. Thus, it is indispensable to reconcile bandwidth reduction against the intended communication frequency.

In summary, this measurement shows that the line-of-sight (LoS) link quality always guarantees the minimum pixel SNR requirement of 10 dB for BER values lower than  $10^{-4}$ . Pixel SNR can be increased to more than 40 dB by setting a longer camera exposure time. However, as mentioned above, a reduction in communication bandwidth must be considered

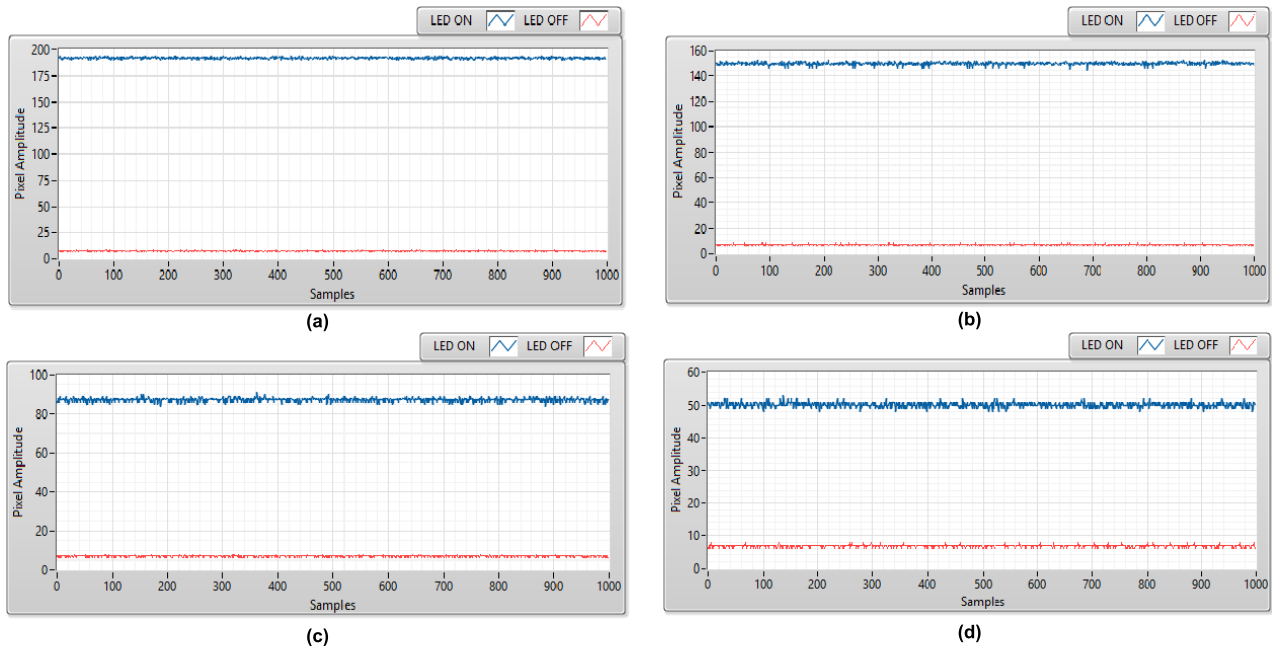


FIGURE 18. Pixel amplitude sampling results at 50 μs exposure time setting using a global shutter camera at different distances: (a) 5m, (b) 10m, (c) 15m, and (d) 20m.

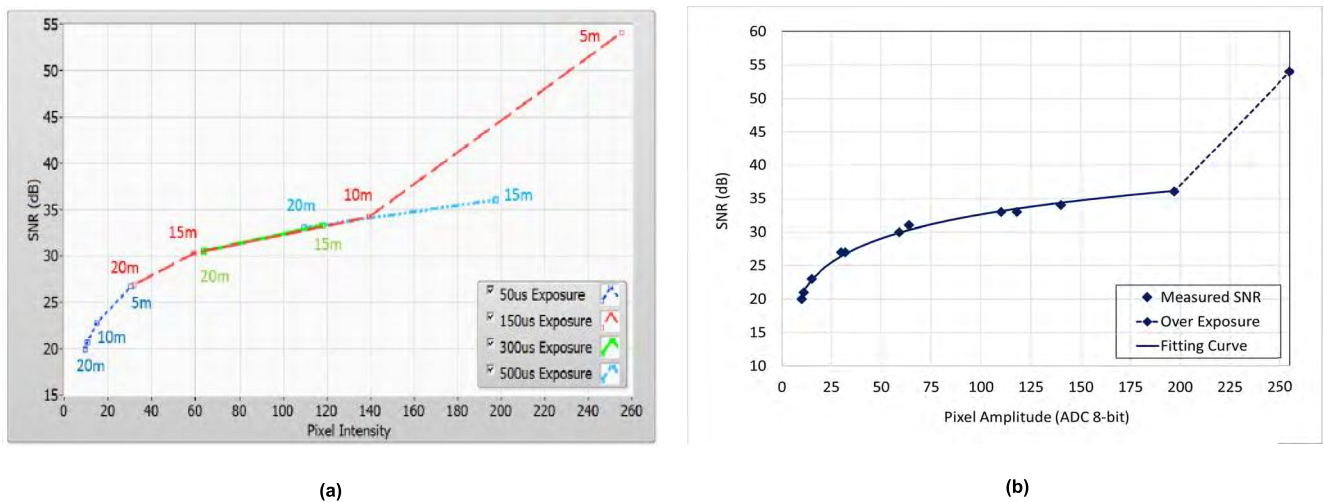


FIGURE 19. (a) Measurement result of pixel SNR versus pixel amplitude using a 2.5 W vehicular lighting model and a rolling shutter camera. (b) Fitting curve for a rolling shutter camera generated from experimental results for a distance range of 5-20m.

carefully. In addition, a long exposure time will increase the probability of occurrence of fuzzy states of LEDs, which occur when samples are obtained during pulse transition. The ratio of fuzzy states must be mitigated by applying FEC to low-rate modulation schemes, such as S2-PSK, or by applying a smart decoding algorithm to high-rate modulation schemes, such as the DS8-PSK waveform.

### 3) ESTIMATION OF S2-PSK BIT ERROR PROBABILITY BASED ON PIXEL SNR

S2-PSK is the spatial approach of the UPSOOK modulation scheme. In UPSOOK, a bit is modulated by performing an

XOR operation between two states of a LED in two different images. Thus, sampling error is caused by a wrong state decision from a pair of input binary states of a LED. Similar to UPSOOK, S2-PSK sampling error occurs only when one of two states of a pair of LEDs is sampled incorrectly. Therefore, the XOR undersampling error probability of either a temporal approach or a spatial approach can be estimated using Equation (13), as shown at the bottom of the next page, where  $p_e$  is the error probability of the LED state decision and  $s_1$  and  $s_2$  are binary states determined from LEDs in an image according to the spatial approach or from adjacent images according to the temporal approach.

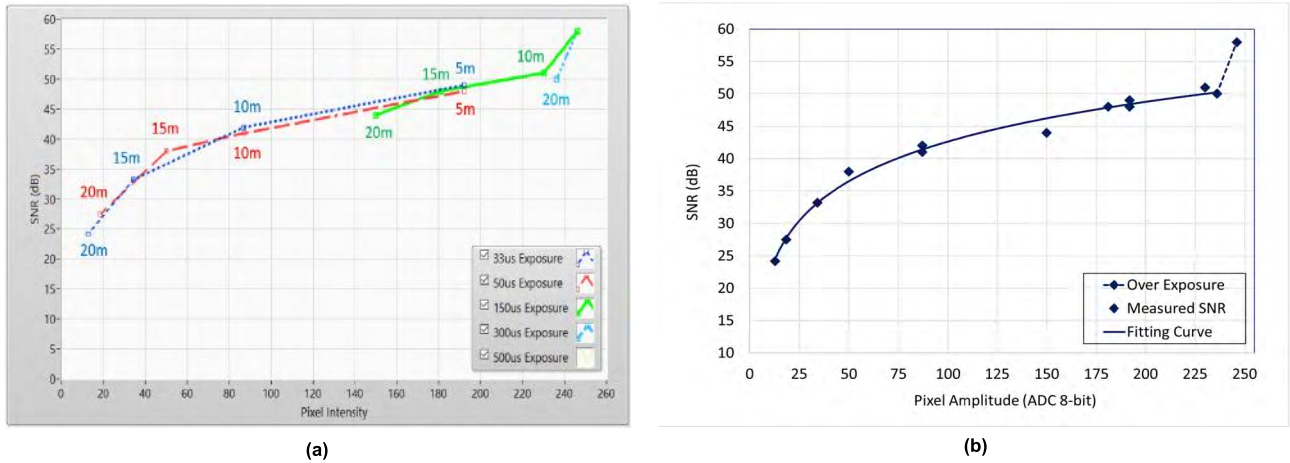


**FIGURE 20.** (a) Measurement result of pixel SNR versus pixel amplitude using a 2.5 W vehicular lighting model and a global shutter camera. (b) Fitting curve for a rolling shutter camera generated from experimental results for a distance range of 5-20m.

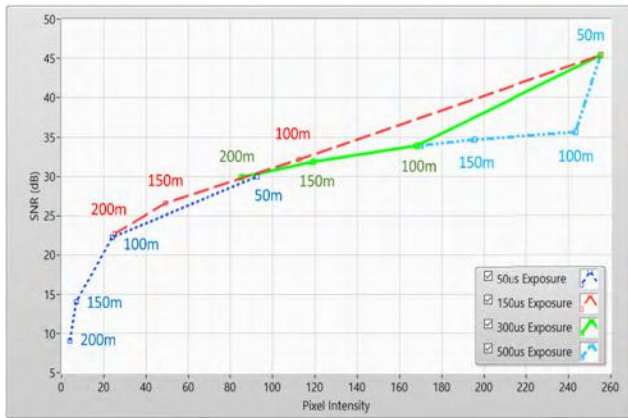


**FIGURE 21.** (a) A 30 W vehicular lighting model; (b) SNR measurement using a rolling shutter camera at a distance of 100m.

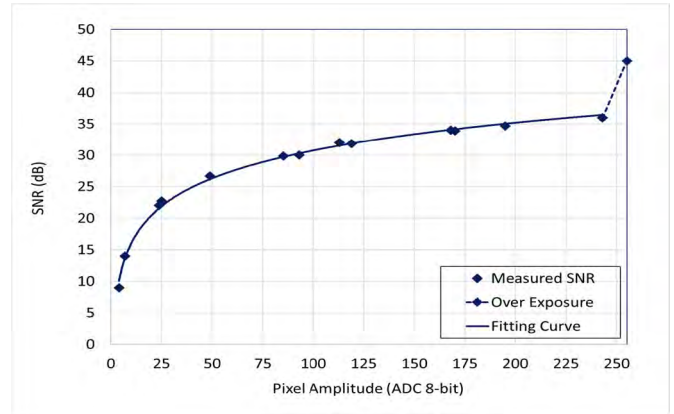
FIGURE 24 shows the estimated curve of S2-PSK bit error probability versus pixel SNR (converted to  $E_b/N_0$ ) in different dimming levels. The graph shows that the modulation schemes require a pixel SNR of at least approximately 10 dB to achieve a BER of  $10^{-6}$ . From the theoretical pixel SNR calculations in FIGURE 12 and the SNR measurements in FIGURE 19, FIGURE 20, FIGURE 22, and FIGURE 23, the requirement of a 10 dB of pixel SNR level for a communication system to achieve a BER  $10^{-4}$  can be satisfied. Therefore, the simulation results prove that the low-rate waveform could be used for tracking RoI with good performance.

AM can be applied to the S2-PSK waveform to generate different levels of average light intensity. With 25% dimming level, S2-PSK requires approximately 20 dB of pixel SNR to achieve a BER of  $10^{-4}$ . With 50% dimming level, S2-PSK requires a pixel SNR of only about 12 dB to achieve a BER of  $10^{-4}$ . The choice of dimming method significantly influences the error probability of sampling LED states for the XOR operation due to the decreased energy level of the Tx signal. Pulse-width modulation (PWM), which was selected as one of the dimming methods for UFSOOK, requires three times the sampling rate than the Tx bit rate to correct the sampling error. On the other hand, AM, which is

$$\begin{aligned}
 P_{e,undersampled\_XOR} &= P(s_1|_{classification=true}, s_2|_{classification=false}) + P(s_1|_{classification=false}, s_2|_{classification=true}) \\
 &= p_e(1 - p_e) + (1 - p_e)p_e \\
 &= 2p_e(1 - p_e)
 \end{aligned} \tag{13}$$

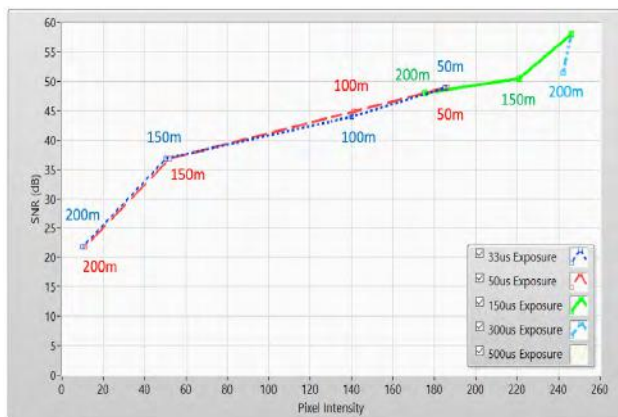


(a)

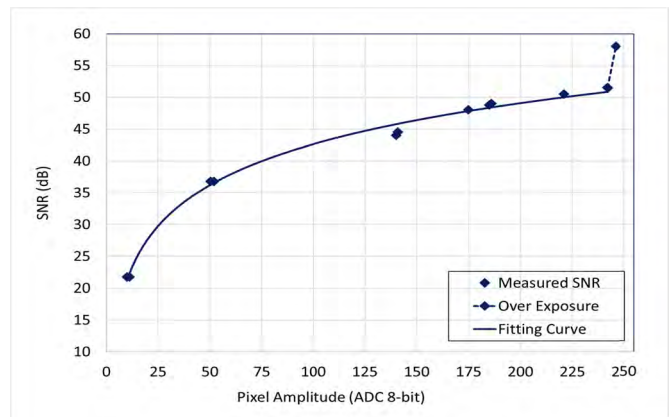


(b)

**FIGURE 22.** (a) Measurement result of pixel SNR versus pixel amplitude using a 30 W vehicular lighting model and a rolling shutter camera. (b) Fitting curve for a rolling shutter camera generated from experimental results for a distance range of 50-200m.



(a)



(b)

**FIGURE 23.** (a) Measurement result of pixel SNR versus pixel amplitude using a 30 W vehicular lighting model and a global shutter camera. (b) Fitting curve for a global shutter camera generated from experimental results for a distance range of 50-200m.

implemented for UPSOOK dimming or S2-PSK dimming, reduces the minimum Euclidean distance between information states. Therefore, the performance of the XOR operation is affected considerably. However, no additional sample is needed for AM dimming when sampling.

#### 4) CAMERA ROTATION ERROR PROBABILITY ESTIMATION

Camera rotation can cause sampling error due to the rolling effect of the Rx rolling shutter camera. The BER probability caused by the bad sampling problem can be estimated using Equation (14) [11] with the assumption that the sampling process is random.

$$p_e \left( \frac{\Delta t}{T} < x \right) = \int_{\frac{\Delta t}{T}=0}^x 4 \times \left( \frac{t_e + \Delta t}{T} \right) d \left( \frac{\Delta t}{T} \right) \quad (14)$$

where  $\Delta t$  is the sampling time deviation, which is calculated using Equation (4),  $T$  is the bit interval,  $x$  determines the

upper limit of the camera’s rotation level (i.e.,  $x = \max(\Delta t/T)$ ), and  $t_e$  is the exposure time of the Rx camera.

The bit error probability can be calculated using Equation (14) and the practical parameters of the proposed system. For example, if an Rx camera’s shutter speed is 10 kHz, its exposure time ( $t_e$ ) is 1/10000 s. The Tx signal is transmitted at an optical clock rate of 1 kHz; thus,  $T$  is 1/1000 s. A temporal repetition code can be applied to Rx transmission as a simple error correction method. In this method, a symbol includes the same three bits. This means a bit is repeatedly transmitted thrice. Therefore, an Rx camera with a typical frame rate of 30 fps can capture each symbol thrice. Then, a voting procedure is applied to decide the output symbol. An output symbol error can occur during the voting procedure if two of the three samples or all three samples from the Rx side are incorrect. Thus, the error probability of the S2-PSK signal with temporally repeated code can be expressed by Equation (15) with the assumption

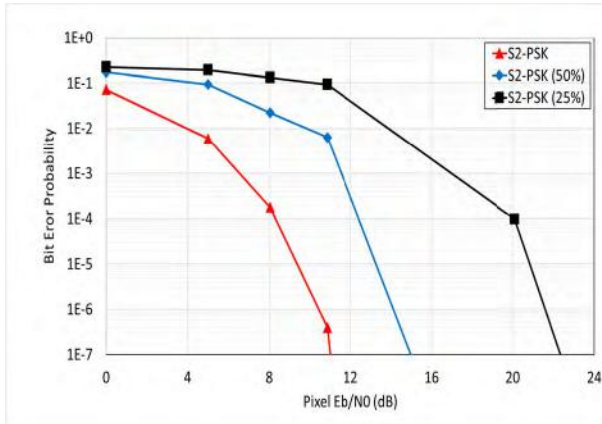


FIGURE 24. Bit error rate probability versus pixel SNR of S2-PSK modulation scheme in different dimming levels.

that the Rx camera sampling rate is three times the Tx bit rate

$$p_{e, \text{repeated\_code}} = p_e^2 \times (1 - p_e) + p_e^3 \quad (15)$$

where  $p_e$  is the error probability of the LED state decision.

FIGURE 25 shows the bit error probability versus rotation level curves of two S2-PSK waveforms, which were sampled using an Rx rolling shutter camera with a shutter speed of 10 kHz, a sampling rate of 34.53 kHz, and a sensor resolution of 1280 × 960 pixels. Equation (4) suggests that if the system uses Tx LEDs with an optical clock rate of 1 kHz and a rolling shutter Rx camera with parameters mentioned above, the number of deviation pixel rows between two LEDs must not exceed more than 34-pixel rows of the image sensor. This means that in the normal vehicular condition and assuming that the distance between two vehicles is 30m, if the Rx camera has a lens with a focal length of 16mm, it is allowed to rotate within 69°. Further distances will allow a wider range of Rx rotation level. From FIGURE 25, it is clear that for a small rotation level (approximately 10% of the maximum camera rotation level), the Rx rolling shutter camera can sample the S2-PSK signal with the repeated code more than ten times better than the S2-PSK signal without the repeated code. Moreover, the rotation problem does not affect the Rx side, which employs the global shutter camera. Therefore, systems with global shutter cameras can offer stable BER performance under the rotation condition.

**B. HIGH-RATE DATA STREAMING MODE**

**1) PERFORMANCE ANALYSIS OF DS8-PSK WAVEFORM**

The proposed DS8-PSK decoder will induce an error by making wrong decisions for each ON/OFF state in a set of LED input states. For example, in the case of 1/8 dimming (12.5% dimming), a wrong set of LED states occurs when the ON-LED is detected as the false OFF-LED, whereas one of the other seven OFF-LEDs is detected as the

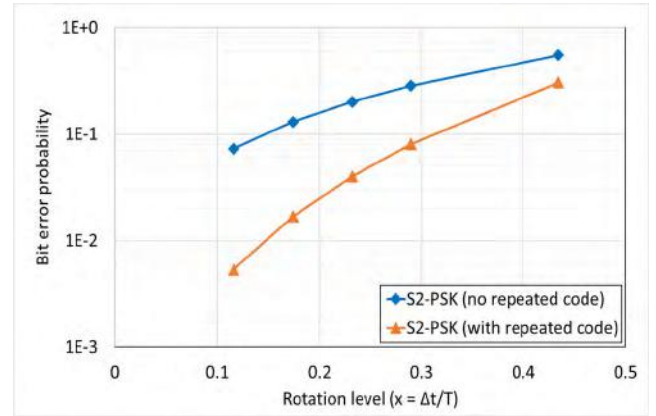


FIGURE 25. Bit error probability versus rotation level of a Rx rolling shutter camera.

false ON-LED. In this case, both LED states are considered to ensure that the average power of all LED states at this sampling time does not change. If the average power does not match the conditions of 12.5% dimming, the decoder can skip this set value. Thus, the sampling error will not be induced. There are seven cases for the switching states of these two LEDs; hence, the error probability for de-mapping can be estimated using Equation (16), as shown at the bottom of this page, where  $p_e$  is the error probability of the LED state classification.

A simulated DS8-PSK system that supports seven dimming levels of transmitted waveforms was implemented. FIGURE 26 shows the simulated BER performance of the DS8-PSK system under the additive white Gaussian noise (AWGN) channel and different dimming levels fitted to the theoretical calculation. In general, the simulated system achieves a BER value of 10<sup>-5</sup> with pixel SNR values of about 18 dB. The novel contribution of the DS8-PSK waveform ensures that the BER performances remain almost unaffected by different dimming levels. The spatial approach takes advantage of the spatial relationship between LEDs on the light source so that the BER can be decreased significantly under dimming.

**2) PERFORMANCE ANALYSIS OF VPPM WAVEFORM**

In VLC, to evaluate the performance of the VPPM waveform for a photodiode (PD) in each dimming level, Equation (17) can be used to estimate the BER when operating the VPPM modulation scheme [20].

$$p_e = \frac{1}{2} \operatorname{erfc} \left( \gamma \sqrt{\frac{E_s}{2N_0}} \sqrt{\frac{d(1-\alpha)}{50}} \right) \quad (17)$$

where  $E_s/N_0$  is the symbol energy to noise power spectral density ratio,  $\gamma$  is the photodiode responsivity,  $d$  is the dimming level ( $0 \leq d \leq 100$ ), and  $\alpha$  is the correlation factor

$$p_{e, \text{demapping}} = 7 \times p (s_{ON} | \text{classification}=\text{OFF}, s_{OFF} | \text{classification}=\text{ON}) = 7p_e^2 \quad (16)$$

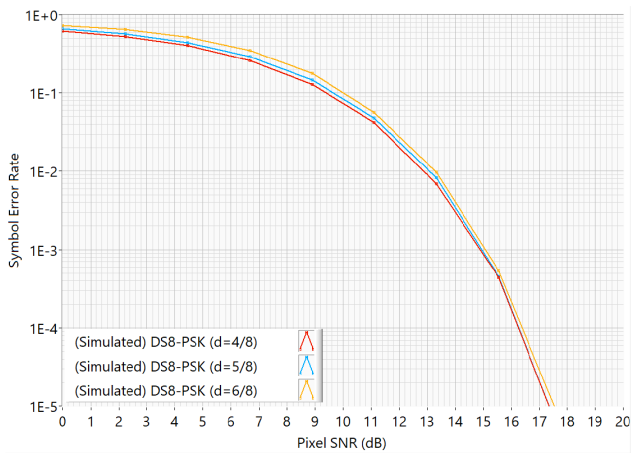


FIGURE 26. Symbol error probability versus pixel SNR of DS8-PSK.

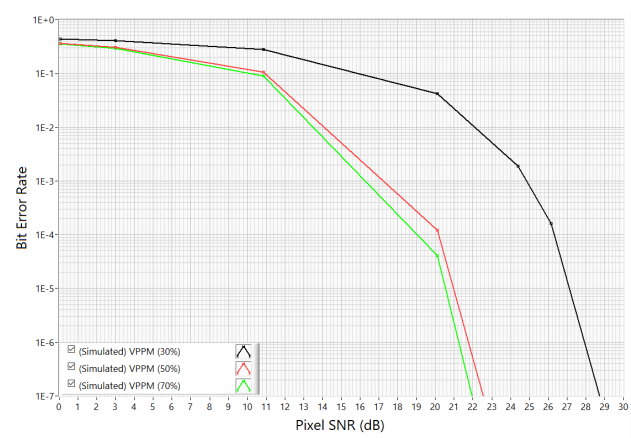


FIGURE 27. Bit error probability versus pixel SNR of VPPM.

of two impulse responses  $q_0(t)$  and  $q_1(t)$ , which are deployed by the receiver through a matched filter process.

In OCC, which does not use matched filtering [17], the BER of the VPPM waveform with pulse-width dimming support in the AWGN channel can be expressed by Equation (18).

$$p_e = \begin{cases} Q\left(\sqrt{\gamma \frac{E_b}{N_0}}\right) & \text{for } 0 < \gamma \leq 0.5 \\ Q\left(\sqrt{(1-\gamma) \frac{E_b}{N_0}}\right) & \text{for } 0.5 < \gamma < 1 \end{cases} \quad (18)$$

where  $\gamma$  is the dimming factor,  $E_b$  is the bit energy, and  $N_0$  is the noise power spectral density.

FIGURE 27 shows the estimation of VPPM BER performance based on pixel SNR from the simulation. The measurements of SNR of the LoS link in our vehicular lighting models shown in FIGURE 19 to FIGURE 23 demonstrate that the requirement of 30 dB SNR can be supported. VPPM showed the best performance at 70% dimming level. It means that when the dimming level is lower, the decrease in allocated signal energy can cause a decrease in transmission performance. Therefore, the dimming levels of VPPM strongly influence the communication performance.

## VI. CONCLUSION AND DISCUSSION

In the present paper, we discussed the technical requirements of OWC/OCC systems for vehicular environments and the potential for implementing a hybrid waveform in these systems. Many technical issues were considered, including tracking of the light source by using a low-frame-rate camera under a high-mobility condition, flicker mitigation, dimming supportability, and frame rate requirement for the high-rate waveform.

The novel contributions of the proposed RoI-signaling waveform and the high-rate data stream concepts can be beneficial when used in a vehicular OWC/OCC system. They not only help users to ensure safe driving in terms of processing time but are also cost-effective. On the other hand, the proposed RoI-signaling waveform S2-PSK was designed as a novel solution to implement on vehicles which already have a pair of light sources in their headlights or tail lights. In addition, the spatial approach to undersampling S2-PSK proved to be a feasible solution for detecting light sources by using a low-frame-rate camera. On the other hand, the high-rate waveform DS8-PSK was designed to support high-resolution dimming without affecting communication performance, which is a novel decoding concept for sampling high-rate waveforms with fuzzy states.

Finally, the results of the numerical experiments and performance analysis showed that the proposed system is technically feasible. With the finalization and release of the IEEE 802.15.7-2018 standard in April 2019, these technical approaches promise to be among the most important communication technologies for the automotive industry in the foreseeable future.

## LIST OF ACRONYMS

AM	Amplitude Modulation
AWGN	Additive White Gaussian Noise
BER	Bit Error Rate
CCD/CMOS	Charge-Coupled Device/Complementary Metal-Oxide Semiconductor
CV	Computer Vision
DS8-PSK	Dimmable-Spatial-8-Phase-Shift-Keying
FEC	Forward Error Correction
HS-PSK	Hybrid-Spatial-Phase-Shift-Keying
IoV	Internet of Vehicles
IoT	Internet of Things
LED	Light-Emitting Diode
LiFi	Light Fidelity
LoS	Line-of-Sight
MIMO	Multiple-Input Multiple-Output
nLoS	non-Line-of-Sight
NN	Neural Network
OCC	Optical Camera Communication
OWC	Optical Wireless Communication
PD	Photodiode
PHY	Physical Layer
PWM	Pulse-Width Modulation

RLL	Run-length Limited Code
RoI	Region-of-Interest
S2-PSK	Spatial-2-Phase-Shift-Keying
SNR	Signal-to-Noise-Ratio
UFSOOK	Undersampled-Frequency-Shift-On-Off-Keying
UPSOOK	Undersampled-Phase-Shift-On-Off-Keying
V2I	Vehicle-to-Infrastructure
V2V	Vehicle-to-Vehicle
V2X	Vehicle-to-Everything
VLC	Visible Light Communication
VPPM	Variable Pulse-Position Modulation
VCPS	Vehicle Cyber Physical System

## REFERENCES

- [1] World Economic Forum White Paper. (2016). *Digital Transformation of Industries: Automotive Industry*. Accessed: Apr. 2019. [Online]. Available: [https://www.accenture.com/t20170411T120057Z\\_w\\_us/en/\\_acnmedia/Accenture/Conversion-Assets/WEF/PDF/Accenture-Automotive-Industry.pdf](https://www.accenture.com/t20170411T120057Z_w_us/en/_acnmedia/Accenture/Conversion-Assets/WEF/PDF/Accenture-Automotive-Industry.pdf)
- [2] A.-M. Căilean and M. Dimian, "Current challenges for visible light communications usage in vehicle applications: A survey," *IEEE Commun. Surveys Tuts.*, vol. 19, no. 4, pp. 2681–2703, 4th Quart., 2017.
- [3] T. Nguyen, A. Islam, T. Hossan, and Y. M. Jang, "Current status and performance analysis of optical camera communication technologies for 5G networks," *IEEE Access*, vol. 5, pp. 4574–4594, Mar. 2017.
- [4] L. U. Khan, "Visible light communication: Applications, architecture, standardization and research challenges," *Digit. Commun. Netw.*, vol. 3, no. 2, pp. 78–88, May 2017.
- [5] J. Gancarz, H. Elgala, and T. D. C. Little, "Impact of lighting requirements on VLC systems," *IEEE Commun. Mag.*, vol. 51, no. 12, pp. 34–41, Dec. 2013.
- [6] T. Nagura, T. Yamazato, M. Katayama, T. Yendo, T. Fujii, and H. Okada, "Improved decoding methods of visible light communication system for its using LED array and high-speed camera," in *Proc. IEEE 71st Veh. Technol. Conf. (VTC)*, Taipei, Taiwan, May 2010, pp. 1–5.
- [7] P. H. Pathak, X. Feng, P. Hu, and P. Mohapatra, "Visible light communication, networking, and sensing: A survey, potential and challenges," *IEEE Commun. Surveys Tuts.*, vol. 17, no. 4, pp. 2047–2077, 4th Quart., 2015.
- [8] X. Ge, H. Cheng, G. Mao, Y. Yang, and S. Tu, "Vehicular communications for 5G cooperative small-cell networks," *IEEE Trans. Veh. Technol.*, vol. 65, no. 10, pp. 7882–7894, Oct. 2016.
- [9] X. Ge, Z. Li, and S. Li, "5G software defined vehicular networks," *IEEE Commun. Mag.*, vol. 55, no. 7, pp. 87–93, Jul. 2017.
- [10] O. Kaiwartya, A. H. Abdullah, Y. Cao, A. Altameem, M. Prasad, C.-T. Lin, and X. Liu, "Internet of vehicles: Motivation, layered architecture, network model, challenges, and future aspects," *IEEE Access*, vol. 4, pp. 5356–5373, Sep. 2016.
- [11] T. Nguyen, A. Islam, and Y. M. Jang, "Region-of-interest signaling vehicular system using optical camera communications," *IEEE Photon. J.*, vol. 9, no. 1, Feb. 2017, Art. no. 7900720.
- [12] T. Nguyen, A. Islam, T. Yamazato, and Y. M. Jang, "Technical issues on IEEE 802.15.7m image sensor communication standardization," *IEEE Commun. Mag.*, vol. 56, no. 2, pp. 213–218, Feb. 2018.
- [13] S. Rajagopal, R. D. Roberts, and S.-K. Lim, "IEEE 802.15.7 visible light communication: Modulation schemes and dimming support," *IEEE Commun. Mag.*, vol. 50, no. 3, pp. 72–82, Mar. 2012.
- [14] *IEEE Standard for Local and Metropolitan Area Network—Part 15.7: Short-Range Wireless Optical Communication Using Visible Light*, IEEE Standard 802.15.7-2011, IEEE-SA, 2011.
- [15] R. D. Roberts, "Undersampled frequency shift ON-OFF keying (UFSOOK) for camera communications (CamCom)," in *Proc. 22nd Wireless Opt. Commun. Conf.*, Chongqing, China, May 2013, pp. 645–648.
- [16] T. Nguyen and Y. M. Jang. (2016). *PHY Sub-Proposal for ISC Using Dimmable Spatial M-PSK (DSM-PSK)*. Accessed: Apr. 2019. [Online]. Available: <https://mentor.ieee.org/802.15/dcn/16/15-16-0015-02-007a-kookmin-university-phy-sub-proposal-for-isc-using-dimmablespatial-mps-k-dsm-psk.pptx>
- [17] R. D. Roberts. (2016). *Intel Proposal in IEEE 802.15.7r1*. Accessed: Apr. 2019. [Online]. Available: <https://mentor.ieee.org/802.15/dcn/16/15-16-0006-01-007a-intel-occ-proposal.pdf>
- [18] P. Luo, Z. Ghassemlooy, H. L. Minh, X. Tang, and H.-M. Tsai, "Undersampled phase shift ON-OFF keying for camera communication," in *Proc. 6th Int. Conf. Wireless Commun. Signal Process. (WCSP)*, Hefei, China, Oct. 2014, pp. 1–6.
- [19] Z. Ghassemlooy, L. N. Alves, S. Zvanovec, and M. A. Khalighi, *Visible Light Communications: Theory and Applications*. Boca Raton, FL, USA: CRC Press, 2017, pp. 107–108.
- [20] J.-H. Yoo and S.-Y. Jung, "Modeling and analysis of variable PPM for visible light communications," *EURASIP J. Wireless Commun. Netw.*, vol. 2013, no. 134, pp. 1–6, May 2013.



**MINH DUC THIEU** received the bachelor's degree in control and automation engineering technology from the Hanoi University of Science and Technology (HUST), Vietnam, in 2015. He is currently pursuing the M.Sc. degree in electrical and electronics engineering with Kookmin University (KMU), South Korea.

His research interests include optical wireless communications (OWC), optical camera communications (OCC), optical V2X communications, and wireless communication systems.



**TUNG LAM PHAM** received the bachelor's degree in control and automation engineering technology from the Hanoi University of Science and Technology (HUST), Vietnam, in 2017. He is currently pursuing the M.Sc. degree in electrical and electronics engineering with Kookmin University (KMU), South Korea.

His research interests include optical wireless communications (owc), optical camera communications (occ), optical V2X communications, neural networks, the Internet of energy, and wireless communication systems.



**TRANG NGUYEN** received the bachelor's degree in biomedical engineering from the Hanoi University of Science and Technology (HUST), Vietnam, in 2013, the M.Sc. and Ph.D. degrees in electrical and electronics engineering from Kookmin University (KMU), South Korea, in 2015 and 2018, respectively.

He is currently a Researcher with the LED Convergence Research Center, KMU. His research interests include optical wireless communications (OWC), optical networks, wireless systems, optical camera communications (OCC), and augmented-reality services via light. He has designed and implemented a variant of OWC/OCC systems. From 2013 to 2018, he has contributed to six international patents/applications and 37 other Korean patents/applications while leading the implementation of over 10 registered software applications; some of these works have been published in several highly cited journal papers. He also leads several projects involving the advanced development of OWC/OCC technologies.

Dr. Nguyen continues as a voting member of IEEE 802.15. He is the creator of OpticalPress.com, a website for discussing OWC/OCC technologies and sharing of open-source softwares.



**YEONG MIN JANG** received the B.E. and M.E. degrees in electronics engineering from Kyungpook National University, South Korea, in 1985 and 1987, respectively, and the Ph.D. degree in computer science from the University of Massachusetts, USA, in 1999.

He was with the Electronics and Telecommunications Research Institute (ETRI), from 1987 to 2000. Since 2002, he has been with the School of Electrical Engineering, Kookmin University (KMU), South Korea, where he has been the Director of the Ubiquitous IT Convergence Center, since 2005, and the Director of the LED Convergence Research Center, since 2010. He served as the Chairman of the IEEE 802.15 Optical Camera Communications Study Group, in 2014. He is currently the Chairman of the IEEE 802.15.7 m Optical Wireless Communications Task Group. He is also the Chairman of the IEEE 802.15 Vehicular Assistive Technology (VAT) Interest Group. His research interests include 5G mobile communications, multi-screen convergence, public safety,

optical wireless communications (OWC), optical camera communications, and the Internet of Things.

Dr. Jang is a Life Member of the Korean Institute of Communications and Information Sciences (KICS). He received a Young Scientist Award from the Korean Government (2003–2006). He has organized several conferences and workshops, such as the International Conference on Ubiquitous and Future Networks (2009–2016), the International Conference on ICT Convergence (2010–2016), the International Conference on Information Networking (2015), and the International Workshop on Optical Wireless LED Communication Networks (2013–2016). He served as the Founding Chair of the KICS Technical Committee on Communication Networks, in 2007 and 2008. He also served as the Executive Director of KICS, from 2006 to 2014, and the Vice President of KICS, from 2014 to 2016. He currently serves as the Co-Editor-in-Chief of *ICT Express*, which is published by Elsevier. He has been the Steering Chair of the Multi-Screen Service Forum, since 2011, and the Society Safety System Forum, since 2015.

• • •